Tellus (1984), *36B*, 367–375

On the efficiency of nucleation scavenging

By JØRGEN B. JENSEN and ROBERT J. CHARLSON, *Environmental Engineering and Science Program, Department of Civil Engineering (FC-05), University of Washington, Seattle, WA 98195, USA*

(Manuscript received September 5, 1983; in final form June 18, 1984)

ABSTRACT

The activation process near cloud base for submicrometer, soluble atmospheric aerosols is described and special attention is focused on the fraction, ε, of the total aerosol mass concentration that form cloud droplets. The variation of ε with updraft speed for various aerosol size distributions is calculated by means of an adiabatic, one-dimensional Lagrangian cloud model. Calculations are made for aerosol particles consisting of pure ammonium bisulphate, $(NH_4)HSO_4$ and the results show that for a clean continental background aerosol population, ε should be very near unity for all updraft speeds. For an average urban aerosol population, ε is close to unity for convective clouds, but for stratiform cases ε decreases rapidly as the updraft velocity is lowered.

1. Introduction

Following its discovery by Whitby et al. (1972), the trimodal mass distribution has been widely observed (Whitby, 1978; Hering et al., 1981). One mass mode is usually found in the diameter (D_p) range between $0.1 < D_p < 1.0$ μm and is almost always the product of some type of condensation. Well-aged, high-temperature condensates, especially soot, are found here, as are products of gas-to-particle conversions at ambient atmospheric temperature (e.g. $SO_4^=$). Another mass mode is found above 1.0 μm diameter and consists largely of mechanically produced materials, e.g. wind-blown soil dust, sea salt, and industrial dusts. A third mode is sometimes found below 0.1 μm due to direct pollution especially by combustion, but in many situations it is subsumed into the $0.1 < D_p < 1.0$ μm mode by Brownian coagulation or due to condensation of gas-phase reaction products. Besides this characteristic trimodal distribution of mass with size, this morphology leads to a strong dependence of chemical composition on size. Fig. 1 shows a typical example of this form of a volume distribution. More recent studies show that this distribution is also a useful representation of the background sulphate aerosol (Lawson and Winchester, 1979; Duce, 1983).

The submicrometer, accumulation mode aerosol is also the primary source of the cloud condensation nuclei (CCN) which are a necessity for formation of warm, unglaciated clouds. This aerosol contributes significantly to the chemical composition of rainwater, most importantly to the content of dissociated species such as sulphate, ammonium, and hydrogen ions (Junge, 1963; Charlson and Rodhe, 1982; Charlson et al., 1983). It has frequently been assumed that much or most of the submicrometer *mass* is effectively incorporated into cloud water (Junge, 1963; Hegg, 1983). However, only meager experimental or theoretical justification of this has been made. A key difficulty in doing so is easily seen upon review of cloud condensation nucleus spectra, or plots of measured (e.g. Twomey, 1977) or calculated (e.g. Junge and McLaren, 1971; Fitzgerald, 1974) *numbers* of particles which are activated when exposed to some supersaturation within a cloud. These are often referred to as supersaturation or just CCN spectra. Unless the mass concentration calculated to be in each size is known to be a realistic representation of actual mass distributions, estimates of the mass of material incorporated into the cloud water are likely to be unrealistic. Because mass depends on size cubed, the uncertainty tends to be large.

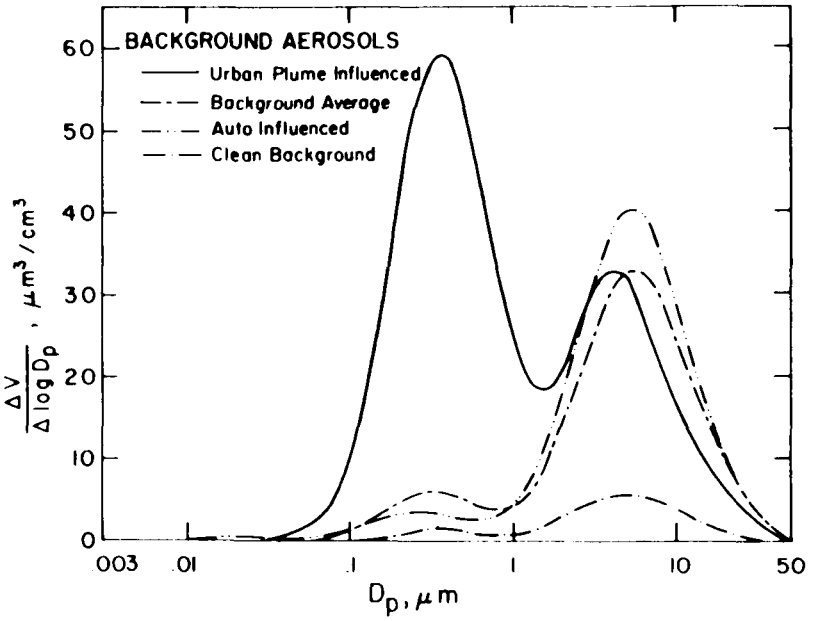

Fig. 1. The mean size distribution of atmospheric aerosols given as log normal volume distributions for four different conditions.

At the same time, studies of the interaction of aerosols and cloud water (e.g. studies of cloud chemistry, scavenging, aerosol life times, or rainwater composition) require a clear understanding of the efficiency with which aerosol *mass* is dissolved in cloud water. It is also necessary to know the sensitivity of this efficiency to the physical and chemical controlling factors (e.g. updraft velocity, liquid water content of the cloud, heterogeneous mixing or entrainment within the cloud, aerosol size distribution, trace gas composition, time available for cloud development, etc.).

Given that the mass distributions that have been directly determined can be represented analytically by a trimodal log normal function (Whitby, 1978), it is possible to calculate another form of supersaturation spectrum. Specifically, we want to calculate the mass fraction of the water soluble submicrometer material that is incorporated into cloud water as functions of the factors controlling supersaturation in a cloud, most especially updraft velocity. Since data are available on the chemical composition of the water-soluble fraction as a function of particle size, this calculation also would allow inference on the expected chemical composition of cloud water.

This sort of calculation is intended to describe the expected chemical consequences of cloud nucleation. Besides this, we will see that it is necessary to use a non-equilibrium description for particle and droplet growth. This general approach will make it possible in the future to include trace gases and their chemical reactions in more advanced models. Ultimately, the production of soluble mass within cloud droplet from chemical reactions of gaseous precursors is expected to result in an important pathway by which aerosols and future CCN are produced from evaporating clouds.

After briefly stating our terminology and the fundamental equations of droplet growth, we present the model for activation of CCN which have a log normal mass distribution. Following the discussion of the numerical procedures, results are presented. Finally, the expected consequences are presented.

2. The model formulation

Numerous studies of clouds have shown that the cloudy air consists both of air that rises through the cloud base and of entrained air. In stratus clouds,

the source of the entrained air is at cloud top. Thermodynamic analysis has shown that contrary to earlier belief, the source of entrained air in cumulus clouds also seems to be at cloud top (Paluch, 1979). The part of the cloud that rises through the cloud base probably has rather large scales (convective clouds $\approx$1 km, frontal stratiform clouds much larger). The turbulent mixing time between cloud base air and entrained air is thus rather long compared to the time it takes to activate aerosol particles and thereby make cloud droplets. In the present formulation, we will therefore confine the discription of the cloud development to the air that enters through the cloud base and is followed only a small distance below and above cloud base. In this initial stage, entrainment can be neglected and the present model therefore includes an adiabatic assumption.

The growth of cloud droplets are determined by the following set of equations. For the growth of droplet radii, r_j, we use a modified version of Fukuta and Walter (1970) expression:

$$\frac{dr_j}{dt} = \frac{1}{r_j} \frac{1 + 0.01S - \exp\left[\frac{2\sigma}{\rho_L R_v T r_j}\right]\left[1 + \frac{im_j M}{W((4\pi/3)\rho_L r_j^3 - mj)}\right]^{\rho_0/\rho_L}}{\frac{L^2}{KR_vT^2} + \frac{R_vT(r_j + \lambda)}{De_s r_j}}. \quad (1)$$

The condensation length, λ, has been added to account for inhomogeneities in the condensation process (Fukuta and Walter, 1970). The curvature term and solution term are somewhat more elaborate than in most cloud models since droplet growth is also followed at subsaturated conditions. The derivation of these two terms follows Mason (1971). S is the supersaturation in %, σ the surface tension of water, R_v is the gas constant for water vapor, and T is the temperature; i is the van't Hoff factor, m_j is the solute mass, M and W the molecular weights of water and solute, L the latent heat of condensation, K is the thermal conductivity of air, and D is the diffusivity of water vapor in air; e_s is the saturation vapor pressure. ρ_o and ρ_L are the densities of pure water and salt solution. The change of water vapor mixing ratio, q_v, is expressed as:

$$\frac{dq_v}{dt} = -\sum_{j=1}^{J} 4\pi\rho_0 n(r_j) r_j^2 \frac{dr_j}{dt}, \quad (2)$$

where $n(r_j)$ is the number of CCN in the j'th class per unit mass of dry air.

For an adiabatic process, the moist static energy, $H = c_pT + Lq_v + gz$ is approximately constant, so the change in temperature can be described by:

$$\frac{dT}{dt} = -\frac{L}{c_p}\frac{dq_v}{dt} - \frac{g}{c_p}\frac{dz}{dt}. \quad (3)$$

Here g is the acceleration of gravity, z is the height, and c_p is the specific heat capacity of dry air.

The approximate rate of change of air density, ρ, is found by differentiating the equation of state for dry air and assuming a hydrostatic balance:

$$\frac{d\rho}{dt} = -\frac{\rho}{T}\frac{dT}{dt} - \frac{\rho g}{R_d T}\frac{dz}{dt}. \quad (4)$$

Here R_d is the gas constant for dry air.

The supersaturation, S, in % is given by:

$$S = 100\left[\frac{q_v}{q_{vs}} - 1\right],$$

where q_{vs} is the saturation mixing ratio at a given temperature. Approximating $q_{vs} \approx 0.622\, e_s/p$, p being the atmospheric pressure, and using the Clausius-Clayperon equation, the hydrostatic equation and the equation of state, give:

$$\frac{dS}{dt} = \frac{(100 + S)}{q_v}\frac{dq_v}{dt} - (100 + S)\left[\frac{L}{R_d T^2}\frac{dT}{dt} + \frac{g}{R_d T}\frac{dz}{dt}\right]. \quad (5)$$

The vertical velocity dz/dt is assumed constant since we confine the study to the shallow layer near cloud base, where the initial cloud-forming processes take place.

3. Aerosol size distributions

The aerosol populations assumed in this study were based on the field measurements by Whitby

Table 1. *Aerosol size distribution specifications*

	Nuclei mode			Accumulation mode		
	D_g* (μm)	σ_g**	Volume ($\mu g\ m^{-3}$)	D_g* (μm)	σ_g**	Volume ($\mu g\ m^{-3}$)
clean continental background	0.03	1.6	0.006	0.35	2.1	1.5
S1	0.03	1.6	0.006	0.35	1.6	1.5
S2	0.03	1.6	0.006	0.35	2.6	1.5
S3	0.03	1.6	0.006	0.25	2.1	1.5
S4	0.03	1.6	0.006	0.45	2.1	1.5
urban average	0.038	1.8	0.63	0.32	2.16	38.4

* D_g is the geometric mean diameter.
** σ_g is the geometric standard deviation.

(1978). Most of our calculations were made with the "clean continental background" size distribution. The sensitivity to variations in the shape of the aerosol spectrum was investigated, and the results using the "clean continental background" size distribution were then compared to Whitby's "urban average" size distribution.

Only the nuclei mode (D_p = 0.01–0.1 μm) and the accumulation mode (D_p = 0.1–1.0 μm) as specified by Whitby were included in the calculations, since they presumably contain the main mass of soluble particles in continental situations. The coarse particle mode ($D_p > 1.0\ \mu m$), consisting mainly of inorganic dust in continental situations was not considered due to its assumed lack of aqueous solubility. Another set of calculations would be needed for marine NaCl with large soluble aerosol particles.

Whitby specifies the size distributions as log normal functions, both as volume and number distributions in terms of geometric mean diameter and geometric standard deviation. The volume distribution was chosen because primarily we wanted to investigate the mass fraction of the activated aerosol particles and because we assumed mass to be directly proportional to volume. The distribution parameters are given in Table 1.

The volume contribution to the total volume from the nuclei mode is clearly insignificant. However, in terms of its contribution to the total number of aerosol particles, it is more important. The main reason for including the nuclei mode was that the aerosol size distribution must at least include all aerosol size classes that may become activated as cloud droplets. In order to have a smooth transition between the nuclei and accumulation mode, both distributions were defined over the whole range D_p = 0.01–1 μm and added. This effectively means that the nuclei mode becomes subsumed into the accumulation mode. For numerical purposes, the composite distributions were discretized into 20 log normally distributed size classes. The aerosols were assumed to consist of soluble ammonium bisulphate, NH_4HSO_4, with a van't Hoff factor, $i = 3$. We note that the calculations are not very sensitive to the value of i. A small mass fraction of small, insoluble particles internally mixed with the soluble material will do little to change our results. In any case, the value of ε for the soluble component is in itself an important question.

4. Initial conditions and numerical procedures

When the vertical velocity at cloud base is small, as in the case of stratiform clouds, one can assume that the droplets formed on CCN are nearly in equilibrium with the surrounding moisture field. In the case of convective clouds with larger vertical velocities at cloud base, this may not always be the case. Mason and Jonas (1974) and Fitzgerald (1974) Overcame this by initiating some of their calculations at a relative humidity of 78% and 95%. However, this introduces numerical instabilities when integrating eqs. (1)–(5) for very small aerosol particles. To avoid these complications, we started the integration at the highest relative humidity where the particles can be assumed to be in equilibrium with the surroundings.

This humidity was found by considering the system time constants, as follows.

Consider a parcel of air moving upwards at some level below cloud base. Let τ_s be the time constant for the change in supersaturation S over a small height interval, and let τ_r be the time constant for the change in drop radius over the corresponding change in height. Then we approximate that:

$$\frac{\Delta S}{\tau_s} = \frac{dS}{dt}, \tag{6}$$

and from eq. (5):

$$\frac{\Delta S}{\tau_s} = \frac{100 + S}{q_v}\frac{dq_v}{dt} - (100 + S)\left[\frac{L}{R_v T^2}\frac{dT}{dt} + \frac{q_v}{R_d T}\frac{dz}{dt}\right].$$

The left-hand side is positive for an upward-moving parcel below cloud base. The first and third terms on the right-hand side are negative, so:

$$\frac{\Delta S}{\tau_s} < -(100 + S)\frac{L}{R_v T^2}\frac{dT}{dz}\frac{dz}{dt},$$

where both sides are positive. When condensation occurs:

$$-\frac{dT}{dz} < \frac{g}{c_p}.$$

So:

$$\tau_s > \frac{\Delta S}{100 + S}\frac{R_v T^2 c_p}{Lgw}, \tag{7}$$

where $w = dz/dt$.

Let Δr be the droplet growth corresponding to the change in supersaturation ΔS. The time constant for drop growth, τ_r, can be approximated by:

$$\frac{\Delta r}{\tau_r} = \frac{dr_j}{dt}. \tag{8}$$

Substituting from eq. (1) and reorganizing leads to:

$$\tau_r = r_j \Delta r \frac{\dfrac{L^2}{KR_v T^2} + \dfrac{R_v T(r_j + \lambda)}{De_s r_j}}{1 + 0.01S - \exp\left[\dfrac{2\sigma}{\rho_L R_v T r_j}\right]\left[1 + \dfrac{im_j M}{W((4\pi/3)\rho_L r_j - m_j)}\right]^{-\rho_w/\rho_L}}. \tag{9}$$

If $\tau_s > \tau_r$, the drop growth is so rapid that the droplets can be considered in equilibrium with the environment. Calculations of τ_s and τ_r for various updraft speeds at $T = 0\,^\circ C$ yields the following results to be used in the model runs: for updraft speeds, w, at and below 25 cm s^{-1}, all aerosol particles including $D_p = 1.0\ \mu m$ can be assumed to be in equilibrium at $S = 0\%$. For higher updraft speeds up to 500 cm s^{-1}, aerosol particles including $D_p = 1.0\ \mu m$ are in equilibrium at $S = -0.25\%$. Thus, for updrafts at or below 25 cm s^{-1}, the calculations are started at $S = 0\%$ and for higher updrafts, the calculations are started at $S = -0.25\%$. All the model runs were made using a cloud base temperature of 0 °C and a cloud base pressure of 900 mb.

5. Discussion

The activation process in an air parcel containing the "clean continental background" aerosol size distribution is shown in Fig. 2. This case might be typical for stratiform clouds with updraft speeds of 20 cm s^{-1} at cloud base. The solution drop size for various particle sizes is shown to grow slowly below cloud base. As the supersaturation goes positive immediately above the cloud base, the particles grow rapidly and activation follows. Note that the activation is reached almost immediately for the small aerosol particles and much later for the large aerosol particles as is implicit in the results of Howell (1949). The fact that larger particles activate later than small particles is unimportant for inertial scavenging processes because the large particles almost immediately above cloud base are of a size where they may be captured by falling precipitation particles. The well-known peak in the supersaturation profile occurs near the point of activation of the smallest aerosol particles. Within the limits of the discreteness of the aerosol size specification, aerosols that have been exposed to supersaturations higher than their critical supersaturation will in fact become activated. The short duration of the supersaturation peak does not

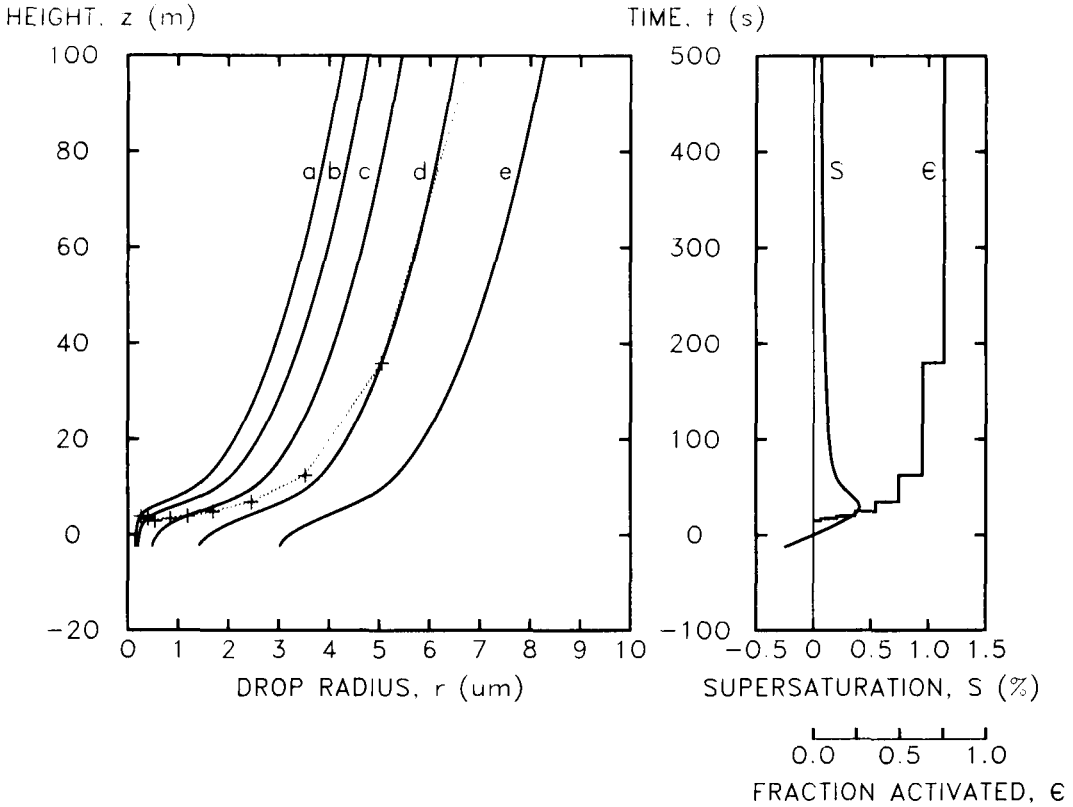

Fig. 2. The activation process of aerosol particles into cloud droplets. The left side of the figure shows the size of solution drops as the aerosol particles activate into cloud drops versus height (or equivalently, time). The vertical velocity is 20 cm s^{-1} and the curves marked a, b, c, d and e represent dry aerosol masses of 3.1×10^{-16}, 6.4×10^{-16}, 5.7×10^{-15}, 1.1×10^{-13} and 9.3×10^{-13} g or equivalently dry particle diameters of 0.070, 0.088, 0.184, 0.484 and 1.00 μm assuming spherical particles. The broken line intersects the individual growth curves where the droplets activate. The figure on the right shows the corresponding supersaturation as a function of height (or time). Note that sharp peak in supersaturation coincides with the activation of the small aerosols. The larger aerosol particles activate at a considerably later time.

hinder any aerosol particles from being activated. The fraction of activated aerosol mass is graphed along with the growth and supersaturation curves. More than 98% of the total aerosol will be activated further up in the cloud, provided the updraft speed is held constant at 20 cm s^{-1}. Thus ε is very close to unity. The largest aerosol particles activate well above 500 m from the cloud base.

The results for a highly convective case is shown in Fig. 3. These are results derived from using the "clean continental background" aerosol size distribution and an updraft speed of 500 cm s^{-1}. The same general pattern appears as for the low updraft case, although a much higher supersaturation peak is evident, which results in a larger fraction of activated aerosol particle mass than in Fig. 2. Thus, the activation of the largest aerosol particles will occur much higher in such clouds.

The activated fraction, ε, of total aerosol mass for various updraft speeds and aerosol size distributions shown in Fig. 4 is very close to unity for all convective cases and most stratiform cases except for very low updraft velocities. This is an important result that is directly applicable to cloud chemistry calculations with parameterized microphysics, e.g. Hegg (1983). The result is not much different when the total aerosol mass is held constant and the geometric mean diameter is grossly perturbed, see Fig. 4.

A very different picture occurs when total

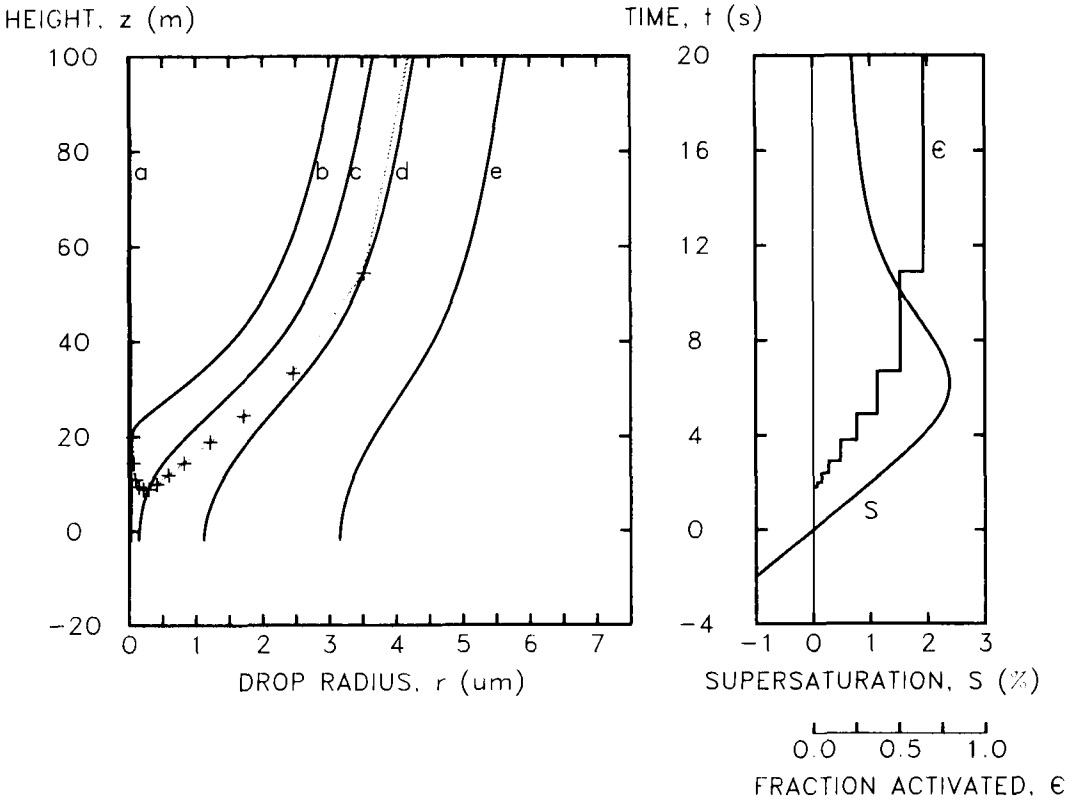

Fig. 3. Same as Fig. 2, but for an updraft speed of 500 cm s^{-1}. The curves labelled a, b, c, d and e corresponds to salt masses of 4.0×10^{-18}, 8.2×10^{-18}, 7.3×10^{-17}, 5.1×10^{-14} and 9.3×10^{-13} g or equivalently dry particle diameters of 0.016, 0.020, 0.042, 0.380 and 1.00 μm assuming spherical particles. Curve (a) pertains to an aerosol size that does not activate, and it is therefore located very close to the z-axis.

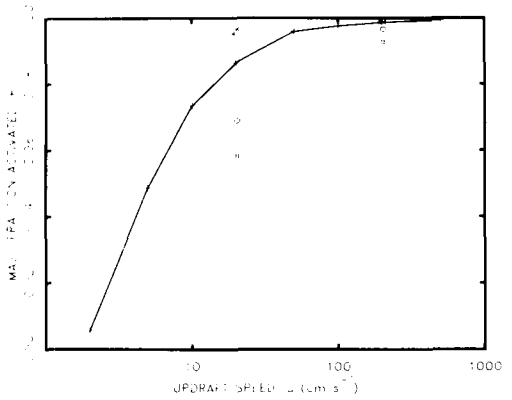

Fig. 4. The fraction ε of the total aerosol mass that is activated into cloud droplets as a function of updraft speed. The data points marked × represent the "clean continental background" size distribution. The symbols ×, #, O, and • represent the perturbed size distributions S1, S2, S3 and S4, see Table 1.

aerosol mass concentration is increased. A comparison between the "clean continental background" (1.5 μg m^{-3}) and the "urban average" (38.4 μg m^{-3}) is shown in Fig. 5. When the aerosol mass concentration is high (38.4 μg m^{-3}), large updraft velocities still result in the activation of most of the aerosol mass. However, in the case of a weak updraft speed such as in a typical stratiform situation, a much smaller fraction of the total aerosol mass gets activated, with the unactivated mass occurring in the small end of the size distribution. The severe dependence of the total activated aerosol mass fraction, ε, on the aerosol load is clearly shown in Fig. 6. The calculations pertain to a population of aerosols with an "urban average" size distribution, but with different total aerosol mass concentrations. An updraft speed of 10 cm s^{-1} typical of stratiform conditions is assumed. This behavior may be typical for situ-

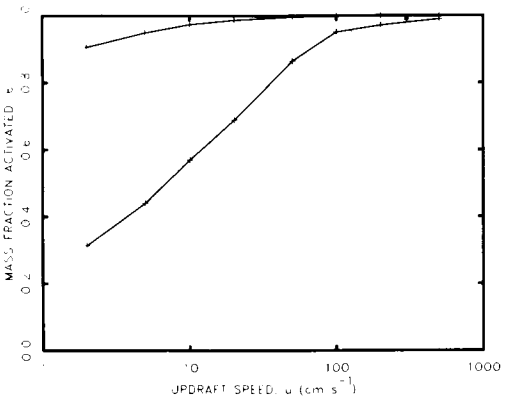

Fig. 5. A comparison of total activated aerosol mass as a function. of updraft speed for different aerosol populations. The upper curve pertains to the "clean continental background" aerosol size distribution, the lower one to the "urban average" size distribution.

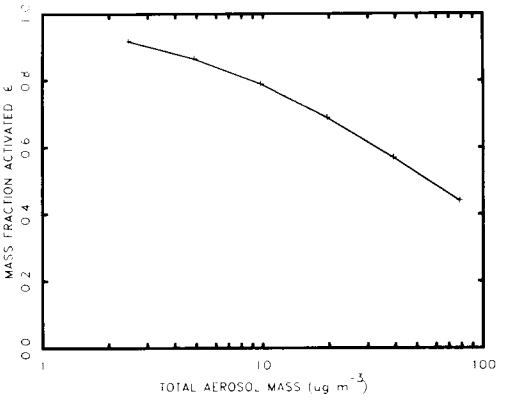

Fig. 6. Total aerosol mass fraction, ε, activated as a function of total aerosol mass. An "urban average" size distribution and an updraft speed of 10 cm s^{-1} is assumed.

ations in which anthropogenic influence is substantial.

To the extent that activation as cloud nuclei is a necessary step prior to scavenging from clouds, it appears possible that significant reduction in the value of ε can occur for high aerosol concentrations in weak updraft situations. This effect should lead to an increase in the atmospheric lifetime of the size classes that are not activated, that is the smallest particle sizes. We also note that these small particles are the least likely to be captured by coalescence with falling drops. Decreased scavenging efficiency due to increases in cloud condensation nuclei mass concentration (and therefore also in total number) may subsequently have a significant effect in determining the rainwater composition. The general sense of this effect is that the increased aerosol mass concentration would lead to increases in the area under influence of the source of the aerosol, perhaps more so than in increased concentration in the rain water itself.

6. Acknowledgements

One of the authors, J.B.J., gratefully wishes to thank the Valle Scandinavian Foundation at the University of Washington and the Fulbright Commission for support for this study.

REFERENCES

Charlson, R. J., Vong, R. and Hegg, D. A. 1983. The sources of sulphate in precipitation (2). Sensitivity to chemical variables. *J. Geophys. Res. 88*, 1375–1377.

Charlson, R. J. and Rodhe, H. 1982. Factors influencing the acidity of natural rainwater. *Nature 295*, 683–685.

Duce, R. A. 1983. Biogeochemical cycles and the air-sea exchange of aerosols, in *the major biochemical cycles and their interactions*. Ed. Bolin, B. and Cook, R. London, Wiley.

Fitzgerald, J. W. 1974. Effect of aerosol composition on cloud droplet size distribution: a numerical study. *J. Atmos. Sci. 31*, 1358–1367.

Fukuta, N. and Walter, A. 1970. Kinetics of hydrometer growth from a water spherical model. *J. Atmos. Sci. 27*, 581–598.

Hegg, D. A. 1983. The sources of sulphates in precipitation (1). Parameterization scheme and physical sensitivities. *J. Geophys. Res. 88*, 1369–1374.

Hering, S. V., Bowen, J. L., Wengert, J. G. and Richards, L. W. 1981. Characterization of the regional haze in the southwestern United States. *Atmos. Environ. 15*, 1999–2009.

Howell, W. E. 1949. The growth of cloud drops in uniformly cooled air. *J. Meteorol. 1*, 134–149.

Junge, C. E. 1963. *Air chemistry and radioactivity*. New York, Academic Press

Junge, C. E. and McLaren, E. 1971. Relationship of cloud nuclei spectra to aerosol size distribution and composition. *J. Atmos. Sci. 28*, 382–390.

Lawson, D. R. and Winchester, J. W. 1979. Atmos-

pheric sulphur aerosol concentrations and characteristics from the south American continent. *Science 205*, 1267–1269.

Mason, B. J. 1971. *The physics of clouds*, 2nd edition. Oxford, Clarendon.

Mason, B. J. and Jonas, P. R. 1974. The evolution of droplet spectra and large droplets by condensation in cumulus clouds. *Q. J.R. Meteorol. Soc. 100*, 23–38.

Paluch, I. R. 1979. The entrainment mechanism in Colorado cumuli. *J. Atmos. Sci. 36*, 2467–2478.

Twomey, S. 1977. Atmospheric aerosols. *Developments in atmospheric sciences, 7.* Amsterdam, Elsevier Scientific Publishing Co.

Whitby, K. T. 1978. The physical characteristics of sulphur aerosols. *Atmos. Environ. 12*, 135–159.

Whitby, K. T. Husar, R. B. and Liu, B. Y. H. 1972. The aerosol size distribution of Los Angeles smog. *J. Colloid Interface Sci. 39*, 237–264.